JOURNAL OF RESEARCH of the National Bureau of Standards—D. Radio Propagation
Vol. 67D, No. 2, March–April 1963

Sunset and Sunrise in the Ionosphere: Effects on the Propagation of Longwaves

Jean Rieker

Contribution from the Swiss Meteorolcgical Office, Zürich (Switzerland)

(Received January 11, 1962; revised October 2, 1962)

The purpose of this study, which is based on photographic recordings showing the phase shift of two signals—i.e., GBR transmitted from Rugby (England) on 16 kilocycles per second and NBA transmitted from Balboa (Panama) on 18 kilocycles per second, both received at the Neuchâtel Cantonal Observatory (Neuchâtel, Switzerland), is twofold:

(1) To investigate the mode of propagation of the GBR and NBA signals.

(2) To study the relation between the time of sunrise, respectively sunset at various ionospheric reflection points and the times at which phase fluctuations appear on the recordings. The author then generalizes the notion of the times of sunrise, respectively sunset by introducing the closely related concept of the zenithal distance Z of the sun at the reflection points considered. Following results published in literature, reflection point altitudes were assumed to be about 70 kilometers during the day. Results were such that:

(a) For the GBR signal; only a one-hop mode is available, night reflection altitudes varying between 88 and 91 kilometers on individual recordings, angles of incidence ϕ on the ground between 7°36′ and 10°25′.

(b) For the NBA signal; a five-hop mode is available, night reflection altitudes varying between 80 and 84 kilometers on individual recordings, angles of incidence ϕ on the ground between 0°27′ and 1°14′.

(c) At sunrise, respectively, sunset, computed zenithal distances for one and the same reflection point at times identical with singularities appearing on successive recordings show a striking analogy.

(d) During one and the same sunrise or sunset, the zenithal distances computed successively for various reflection points and related to singularities read on a same recording present also a striking analogy.

(e) The time of onset of ionizing radiation at all night reflection points seems to be of major importance for both the propagations of the GBR and NBA signals. During sunset, the altitude of the day reflection point which was stabilized at around 70 kilometers increases as soon as the zenithal distance of the sun exceeds 90°. At sunrise, on the other hand, the altitude of the reflection point stabilizes at around 70 kilometers, when the zenithal distances of the sun reach or go below 90°.

(f) In the case of the NBA signal a phase fluctuation already occurs at a zenithal distance of about 103°, especially at sunrise. At that moment, the distance between the reflection point and the layer formed by the ionizing radiations of the sun is about 100 kilometers.

(g) At sunrise, the curves showing the energy of the received signals display the following features:

For a one-hop mode (Rugby), a momentary strong absorption when the reflection point altitude reaches 82 kilometers; in the case of several ionospheric reflections (Balboa), a succession of absorption lines corresponding to the successive diminishing of the altitude of the ionospheric reflection points.

(h) At sunset, the interpretation of the energy is more delicate:

For a one-hop mode (Rugby), a momentary increase occurs in the energy of the signal before the night level of reflection is reached; in the case of a five-hop mode (Balboa), the interpretation of the absorption curve is difficult because five ionospheric reflection points change their altitude and the resulting phase fluctuations become entangled.

1. Introduction

A simple geometrical model explaining the transition from night-to-day propagation resulted from a previous experimental study [Rieker, 1960]. The model assumed longwave propagation in successive hops in the waveguide formed by the earth and the lower edge of the ionospheric layer. Implicit in this was the assumption that the angles of incidence on the ground are constant for a definite wavepath.

Atmospherics emanating from the same azimuth had been picked up on the loop aerial of a narrow-sector direction finder pointed toward the source; these receptions were analyzed from recordings.

This study confirmed a view previously held, that reflection-point altitudes are higher at night than during daylight hours. Moreover, it became possible to distinguish mixed propagation paths from all-night propagation or all-day propagation. It was also found that angles of incidence on the ground are very small, varying between 0 and 2 to 3°.

In the meantime, theoretical studies, especially Wait's fundamental "Diffraction Theory for LF Skywave Propagation" [Wait, 1961; Wait and Conda, 1961], indicate that the angles of incidence on the ground should be in excess of about 5° for a 27 kc/s wave frequency if geometrical optics are strictly valid. Despite violations of this condition, geometrical optical arguments are often used. From a qualitative viewpoint, the final conclusion should be valid. For a more refined treatment, rigorous mode theory should be used [Wait, 1962]. For example, it was found in the study mentioned above [Rieker, 1960] that 27 kc/s waves emanating from distant thunderstorms (sferics) are received at angles of incidence on the ground less than 2 or 3°, the mode of propagation being the simplest possible, as previously suggested by Wait [1959].

Obviously, the method used in investigating distant thunderstorm emissions cannot be applied at sunset. Narrow-sector direction finder recordings [Rieker, 1960, (figs. 1 and 2)] show that these sources, when recorded at night, usually cannot be located during daytime, at least as far as more distant thunderstorms are concerned. This results in major difficulties when an attempt is made during the day to determine the azimuth of areas of thundery

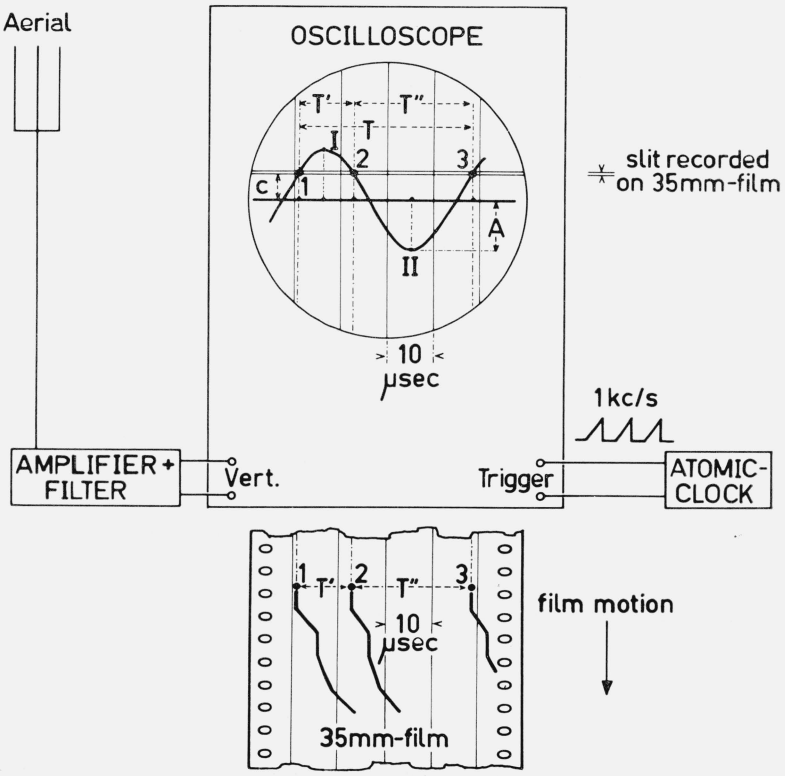

FIGURE 1. *A diagram of the photographic method used at the observatory of Neuchâtel for the registration of the phase fluctuations of the GBR signal (Rugby) and NBA signal (Balboa).*

Accuracy of the atomic clock: 1 part in 10^{11}. Frequency difference between oscillator in Balboa and atomic clock in Neuchâtel always smaller than 2 parts in 10^{10} (i.e., 17 μsec per 24 hr).

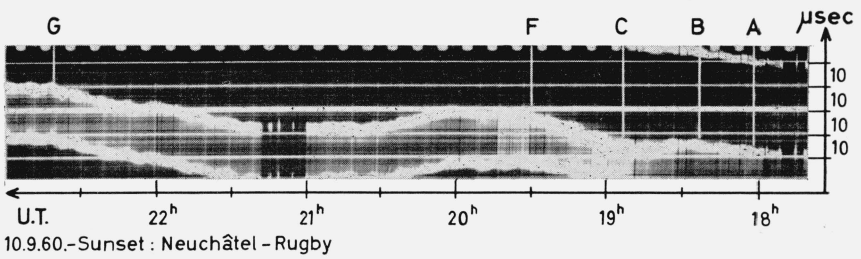

FIGURE 2. *Phase fluctuations of the GBR signal at sunset on the Sept. 10, 1960.*

Discontinuities *A*, *B*, *C*, *F*, and *G* are recorded in table 12.

activity to be recorded the following night. Furthermore, it is impossible to check selected azimuths without operating a narrow-sector direction finder under normal conditions.

Here we propose to reinvestigate the problem of longwave propagation by another method: the analysis of phase fluctuations of a signal (Rugby GBR or alternatively Balboa NBA) with respect to a local frequency standard (atomic clock at Neuchâtel).

Scrutiny of recordings kindly supplied by Dr. J. Bonanomi, Director of Neuchâtel Observatory, revealed the possibility of some conclusions about longwave propagation at sunrise and sunset.

2. Instrumentation and Recording

As a check against the frequency of the Neuchâtel standard (atomic) clock, the Neuchâtel Observatory (47°00′—06°57′E) receives signals from Station GBR, Rugby, England (52°22′ N—01°11′ W) and Station NBA, Balboa, Panama (09°03′N—79°39′W). These frequencies are intercompared (fig. 1) by means of a filmed record of the oscilloscope trace, which is triggered by the Neuchâtel reference signal.

The cathode tube screen shows a fixed sinusoid when the phase difference is constant. At sunrise and sunset, the length of the signal path is modified by the change in altitude of the ionospheric reflections points. A phase lag at sunset is indicated by a shifting of the sinusoid, with an equal and opposite shift at sunrise. Filming of this sinusoid shift at two or three points (1, 2, 3) of identical ordinate c results in nearly parallel traces, as shown in figure 1.

Let $T=\frac{1}{\nu}$ be the period of the sinusoid, where ν is the frequency of the received wave, $\omega=2\pi\nu$ is the gyratory frequency, and c is the distance from the slit to the abscissa. The following equation expresses the sinusoid on the oscilloscope screen:

$$u=\frac{c}{\cos\frac{\omega T'}{2}}\cos\left[\omega t-\omega\left(t_1+\frac{T'}{2}\right)\right] \qquad (1)$$

where

$$t_I=t_1+\frac{T'}{2} \qquad \text{(fig. 1)} \qquad (2)$$

T' is expressed in microseconds and is related to the period by the equation

$$T=T'+T''.$$

The square of amplitude

$$A^2=\frac{c^2}{\cos^2\frac{\omega T'}{2}} \qquad (3)$$

reveals the behavior of the received wave energy.

When S designates the total path traveled by the wave after completion of n successive hops, the length difference ΔS between the day and night paths is derived easily from the equation giving the phase:

$$\delta=\omega\left(t_1+\frac{T'}{2}\right),$$

which can be written

$$\delta=2\pi\frac{S}{\lambda},$$

and finally

$$\Delta S=v\Delta\left(t_1+\frac{T'}{2}\right). \qquad (4)$$

v being the velocity of propagation of the signal, i.e., 3.10^5 km/sec=velocity of light.

The accuracy of the atomic clock is 1 part in 10^{11}. The frequency difference between the oscillator in Balboa and the atomic clock in Neuchâtel never exceeds 2 parts in 10^{10} (i.e., 17 μsec per 24 hr).

Four recordings of the phase fluctuations of the GBR signal (figs. 2, 3, 4, and 5), and five recordings of the phase shifts of the NBA signal (figs. 6, 7, 8, 9, and 10) were studied. These recordings are among the first made at the Neuchâtel Observatory during initial trials, which explains the two different scales used for time registration.

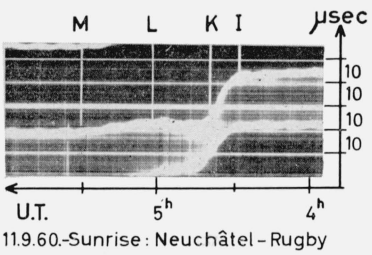

FIGURE 3. *Phase fluctuations of the GBR signal at sunrise on the Sept. 11, 1960.*

Discontinuities I, K, L, and M are recorded in table 10.

3. Computation of the Length Difference ΔS (km) Between the Day and Night Paths

3.1. Rugby

For Rugby, the period of the sinusoidal wave is

$$T=T'+T''=62{,}5\ \mu\text{sec}.$$

The following values were obtained when computing the differences $\Delta S=vt_I$ (4) between the fixed points $A-G$, figures 2 and 4, for sunset, and $I-M$, figures 3 and 5, for sunrise:

Figure 2, sunset	$\Delta t_I=31$ μsec,	$\Delta S=9{,}3$ km
Figure 4, sunset	$\Delta t_I=28$ μsec,	$\Delta S=8{,}4$ km
Figure 3, sunrise	$\Delta t_I=28$ μsec,	$\Delta S=8{,}4$ km
Figure 5, sunrise	$\Delta t_I=26$ μsec,	$\Delta S=7{,}8$ km.

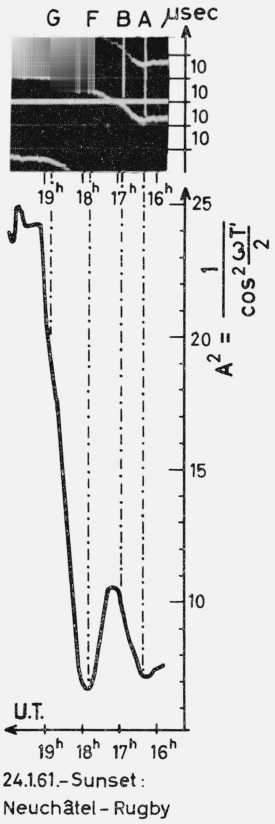

FIGURE 4. *Phase fluctuations of the GBR signal at sunset on the Jan. 24, 1961.*

Discontinuities A, B, F, and G are recorded in table 12. The square of the amplitude of the signal represented below has been calculated from the time difference T', resp. T'' in μsec, (see also fig. 1).

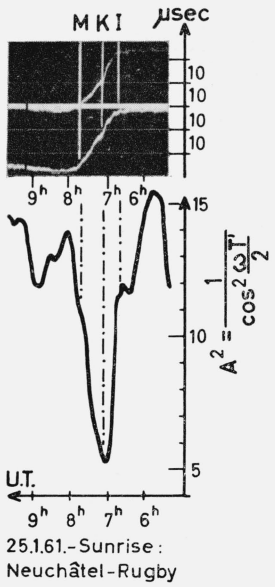

FIGURE 5. *Phase fluctuations of the GBR signal at sunrise on the Jan. 25, 1961.*

Discontinuties I, K, and M are recorded in table 10. The square of the amplitude of the signal represented below has been calculated from the time difference T' in μsec, (see also fig. 1).

Computation of the path length differences assumes a signal propagation velocity equal to the velocity of light.

3.2. Balboa

For Balboa, the period of the sinusoidal wave is

$$T = T' + T'' = 55{,}55 \ \mu\text{sec}.$$

Since these recordings (figs. 7 and 9) were interrupted before sunrise had occurred over the complete path Neuchâtel-Balboa, they cannot be considered for the time being. The following values were obtained when computing the differences $\Delta S = vt_I$ (4) between the fixed points A_1 and F^*_5, figure 6, B_1 and F_5, figure 8, and A^*_1 and G_5, respectively H_1 and P_5, figure 10:

Figure 6, sunset $\Delta t_I = 59$ μsec, $\Delta S = 17{,}7$ km
Figure 8, sunset $\Delta t_I = 49$ μsec, $\Delta S = 14{,}7$ km
Figure 10, sunset+sunrise $\Delta t_I = 71$ μsec, $\Delta S = 21{,}3$ km.

4. Determination of the Mode of Propagation

4.1. Altitudes of the Day Reflection Layer

In order to determine the mode of propagation of the signal, the altitudes of either the day or night reflection points must be known. Since neither can be found in this study, reference was made to results of previous research found in literature indicating an altitude of day reflection layer of about 70 km [Budden, Ratcliffe, and Wilkes, 1939; Bracewell and Kruse, 1951; Nertney, 1953; Gregory, 1956; Revellio, 1956; Wait, 1959].

This being assumed, nocturnal reflection altitude computations were based on the values of ΔS deduced from the readings of Δt_I on the recordings (4).

4.2. Mode of the Rugby GBR Signal Propagation

Table 1 provides ΔS values as computed for a one-hop mode, figure 11, and for a two-hop mode. For the particular case of only one ionospheric reflection two neighboring reflection altitudes were selected, $H = 88$ km and $H = 90$ km.

TABLE 1. *Neuchâtel—Rugby*

(Geocentrical angle: $\theta_f = 7°30'$)

	H	Geocentrical angle θ	Angle of incidence on the ground ϕ	s	$S = \Sigma s$	ΔS
	km			km	km	km
1 Ionspheric reflection	70	3°45′	7°36′	424, 99	849, 98	0
	88	3°45′	9°57′	428, 89	857, 79	7, 81
	90	3°45′	10°13′	429, 37	858, 74	8, 76
2 Ionspheric reflections	70	1°52,5′	17°28′	220, 93	883, 72	0
	90	1°52,5′	22°12′	228, 33	913, 32	29, 60

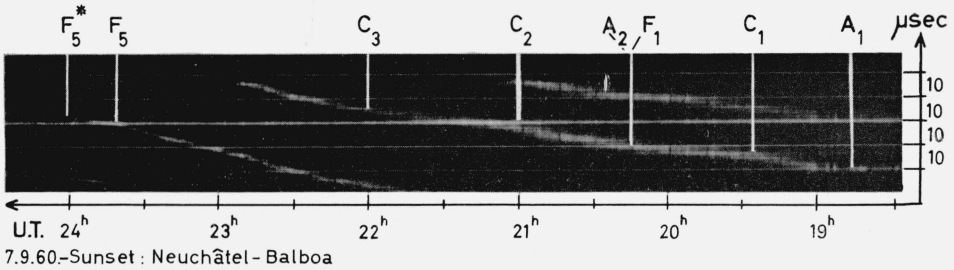

FIGURE 6. *Phase fluctuations of the NBA signal at sunset on the Sept. 7, 1960.*
Discontinuities are recorded in table 16.

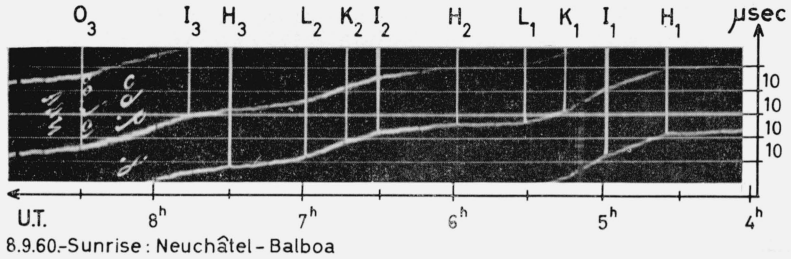

FIGURE 7. *Phase fluctuations of the NBA signal at sunrise on the Sept. 8, 1960.*
Discontinuities are recorded in table 14. The sunrise-effect continues after the interruption of the record at 9 UT.

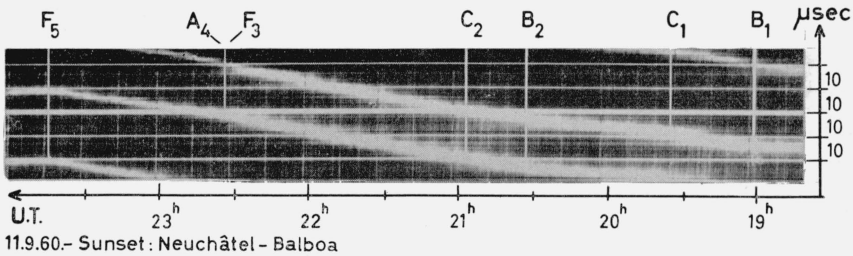

FIGURE 8. *Phase fluctuations of the NBA signal at sunset on the Sept. 11, 1960.*
Discontinuities are recorded in table 16.

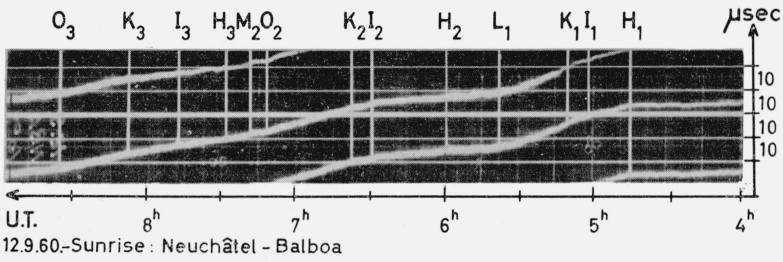

FIGURE 9.—*Phase fluctuations of the NBA signal at sunrise on the Sept. 12, 1960.*
Discontinuities are recorded in table 14. The sunrise-effect continues after the interruption of the record at 9 UT.

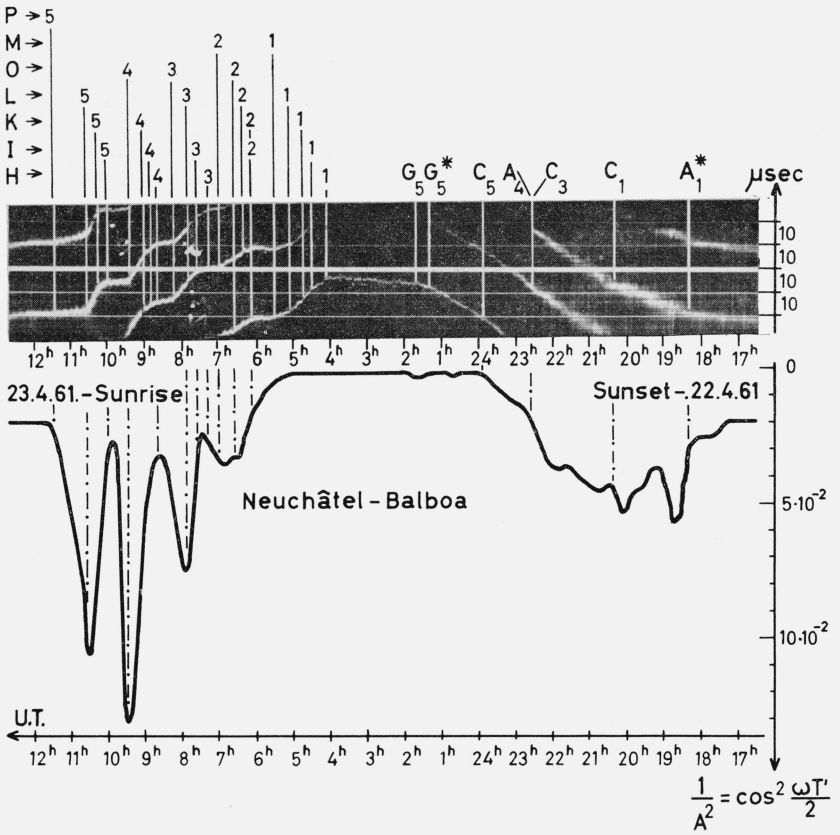

FIGURE 10.—*Phase fluctuations of the NBA signal at sunset on the April 22, 1961 and at sunrise on the April 23, 1961.*

Discontinuities are recorded in table 16 and table 14. The inverse square of the amplitude of the signal represented below has been calculated from time difference T', resp. T'' in μsec, (see also fig. 1).

It can be ascertained that if a one-hop mode occurs, the difference ΔS=7,81 km, respectively 8,76 km is comparable with the differences deduced from the recordings (see sec. 3.1) and are between 7,8 km and 9,3 km. Angles of incidence ϕ on the ground meet Wait's requirement [Wait, 1961].

A two-hop mode would result in a difference in the path traveled by the signal about 3,5 times larger. This possibility can therefore be excluded as well as that one of two-hops during the day and one-hop during the night or inversely.

Ultimately therefore, the mode of propagation of the GBR signal received at Neuchâtel is also only a one-hop mode, night reflection altitude varying between 88 and 91 km for a day reflection altitude assumed to be at 70 km.

4.3. Mode of the Balboa NBA Signal Propagation

a. Method

The characteristic elements relating to the path Neuchâtel-Balboa are shown in table 2. These elements were computed for 5, 6, and 7 hops and also to a certain extent for 8 hops. The altitude of the day reflection point was taken as 70 km while two night reflection altitudes—i.e., 90 and 84 km—were considered. The column headed "5 ionospheric re-

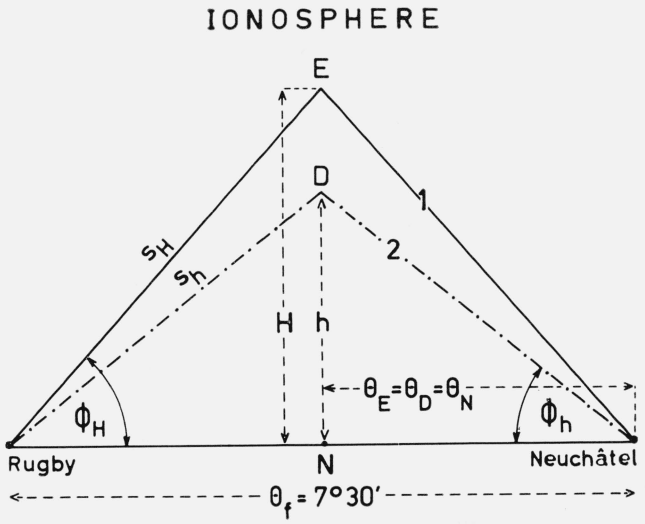

FIGURE 11. *Model of the propagation between Rugby and Neuchâtel in the case of a one-hop skywave (night propagation 1, day propagation 2).*

TABLE 2. *Neuchâtel—Balboa*

(Geocentrical angle: $\theta_f = 81°05'$)

	No. (fig. 12)	Straight line equation	Night reflection $H=90$ km, Day reflection $h=70$ km: Angle of incidence on the ground ϕ	Geocentrical angle		s	$S=\Sigma s$	ΔS	Night reflection $H=84$ km, Day reflection $h=70$ km: Angle of incidence on the ground ϕ	Geocentrical angle		s	$S=\Sigma s$	ΔS
					of the last night reflection point						of the last night reflection point			
						km	*km*	*km*				*km*	*km*	*km*
		$10\ \theta_H = 81°05'$	1°36′	$\theta_{90} = 8°06'30''$	$\theta_{E_1^1} = 8°06'30''$	911, 65	9116, 5	0	1°14′	$\theta_{84} = 8°06'30''$	$\theta_{E_1^1} = 8°06'30''$	910, 66	9106, 6	0
5 Ionospheric reflections	1	$2\theta_{70} + 8\theta_H = 81°05'$	1°21′	$\theta_{70} = 7°16'30''$ $\theta_{90} = 8°19'00''$	$\theta_{E_1^2} = 22°52'00''$	815, 5 935, 0	9111	6±3	1°05′	$\theta_{70} = 7°30'30''$ $\theta_{84} = 8°15'30''$	$\theta_{E_1^2} = 23°15'30''$	841, 5 927, 0	9099	8±3
	2	$4\theta_{70} + 6\theta_H = 81°05'$	1°07′	$\theta_{70} = 7°28'15''$ $\theta_{90} = 8°32'00''$	$\theta_{E_1^3} = 38°25'00''$	837, 3 958, 5	9100	17±3	0°55′	$\theta_{70} = 7°39'30''$ $\theta_{84} = 8°24'30''$	$\theta_{E_1^3} = 39°02'30''$	858, 0 944, 0	9098	9±3
	3	$6\theta_{70} + 4\theta_H = 81°05'$	0°53′	$\theta_{70} = 7°41'00''$ $\theta_{90} = 8°44'45''$	$\theta_{E_1^4} = 54°46'45''$	861, 0 982, 0	9094	23±3	0°46′	$\theta_{70} = 7°48'15''$ $\theta_{84} = 8°33'45''$	$\theta_{E_1^4} = 55°23'15''$	874, 5 961, 0	9090	17±3
	4	$8\theta_{70} + 2\theta_H = 81°05'$	0°38′	$\theta_{70} = 7°53'30''$ $\theta_{90} = 8°58'30''$	$\theta_{E_1^5} = 72°06'30''$	884, 0 1007, 5	9087	30±3	0°35′	$\theta_{70} = 7°57'30''$ $\theta_{84} = 8°43'00''$	$\theta_{E_1^5} = 72°22'20''$	891, 5 978, 0	9086	21±3
		$10\theta_{70} = 81°05'$	0°27′	$\theta_{70} = 8°06'30''$		908, 50	9085, 0	31, 5	0°27′	$\theta_{70} = 8°06'30''$		908, 50	9085, 0	21, 6
6 Ionospheric reflections		$12\theta_H = 81°05'$	3°25′	$\theta_{90} = 6°45'25''$	$\theta_{E_1^1} = 6°45'25''$	761, 53	9138, 4	0	2°58′	$\theta_{84} = 6°45'25''$	$\theta_{E_1^1} = 6°45'25''$	760, 50	9126, 0	0
	5	$2\theta_{70} + 10\theta_H = 81°05'$	3°10′	$\theta_{70} = 5°53'00''$ $\theta_{90} = 6°56'00''$	$\theta_{E_1^2} = 18°42'00''$	660, 5 781, 0	9129	9±3	2°47′	$\theta_{70} = 6°08'30''$ $\theta_{84} = 6°52'45''$	$\theta_{E_1^2} = 19°09'45''$	689, 5 774, 5	9125	1±3
	6	$4\theta_{70} + 8\theta_H = 81°05'$	2°54′	$\theta_{70} = 6°03'15''$ $\theta_{90} = 7°06'30''$	$\theta_{E_1^3} = 31°19'30''$	680, 0 800, 5	9124	14±3	2°36′	$\theta_{70} = 6°15'45''$ $\theta_{84} = 7°00'15''$	$\theta_{E_1^3} = 32°03'15''$	703, 0 788, 5	9120	6±3
	7	$6\theta_{70} + 6\theta_H = 81°05'$	2°40′	$\theta_{70} = 6°13'20''$ $\theta_{90} = 7°17'15''$	$\theta_{E_1^4} = 44°38'15''$	698, 5 820, 5	9115	23±3	2°26′	$\theta_{70} = 6°22'30''$ $\theta_{84} = 7°08'15''$	$\theta_{E_1^4} = 45°23'15''$	715, 5 804, 0	9118	8±3
	8	$8\theta_{70} + 4\theta_H = 81°05'$	2°24′	$\theta_{70} = 6°24'00''$ $\theta_{90} = 7°28'15''$	$\theta_{E_1^5} = 58°40'15''$	718, 0 841, 0	9108	30±3	2°16′	$\theta_{70} = 6°30'00''$ $\theta_{84} = 7°16'15''$	$\theta_{E_1^5} = 59°16'15''$	729, 5 818, 0	9108	18±3
	9	$10\theta_{70} + 2\theta_H = 81°05'$	2°02′	$\theta_{70} = 6°34'45''$ $\theta_{90} = 7°38'45''$	$\theta_{E_1^6} = 73°26'15''$	738, 0 860, 0	9100	38±3	2°06′	$\theta_{70} = 6°37'45''$ $\theta_{84} = 7°23'45''$	$\theta_{E_1^6} = 73°40'45''$	743, 5 832, 5	9100	26±3
		$12\theta_{70} = 81°05'$	1°57′	$\theta_{70} = 6°45'25''$		758, 27	9099, 3	39, 1	1°57′	$\theta_{70} = 6°45'25''$		758, 27	9099, 2	26, 8
7 Ionospheric reflections		$14\theta_H = 81°05'$	4°57′	$\theta_{90} = 5°47'30''$	$\theta_{E_1^1} = 5°47'30''$	654, 43	9162, 0	0	4°31′	$\theta_{84} = 5°47'30''$	$\theta_{E_1^1} = 5°47'30''$	653, 42	9147, 6	0
	10	$2\theta_{70} + 12\theta_H = 81°05'$	4°41′	$\theta_{70} = 5°00'45''$ $\theta_{90} = 5°55'15''$	$\theta_{E_1^2} = 15°56'45''$	564, 5 669, 0	9158	4±3	4°18′	$\theta_{70} = 5°13'00''$ $\theta_{84} = 5°53'15''$	$\theta_{E_1^2} = 16°19'15''$	586, 0 664, 5	9146	2±3
	11	$4\theta_{70} + 10\theta_H = 81°05'$	4°27′	$\theta_{70} = 5°08'00''$ $\theta_{90} = 6°03'15''$	$\theta_{E_1^3} = 26°35'15''$	578, 0 684, 0	9153	9±3	4°07′	$\theta_{70} = 5°18'45''$ $\theta_{84} = 5°59'00''$	$\theta_{E_1^3} = 27°14'00''$	597, 5 675, 5	9145	3±3
	12	$6\theta_{70} + 8\theta_H = 81°05'$	4°15′	$\theta_{70} = 5°15'30''$ $\theta_{90} = 6°11'30''$	$\theta_{E_1^4} = 37°44'30''$	591, 5 699, 0	9141	21±3	3°52′	$\theta_{70} = 5°24'30''$ $\theta_{84} = 6°04'45''$	$\theta_{E_1^4} = 38°31'45''$	608, 5 686, 0	9139	9±3
	13	$8\theta_{70} + 6\theta_H = 81°05'$	4°01′	$\theta_{70} = 5°22'45''$ $\theta_{90} = 6°20'30''$	$\theta_{E_1^5} = 49°22'30''$	605, 0 715, 5	9133	29±3	3°48′	$\theta_{70} = 5°30'00''$ $\theta_{84} = 6°11'00''$	$\theta_{E_1^5} = 50°11'00''$	619, 5 696, 5	9134	14±3
	14	$10\theta_{70} + 4\theta_H = 81°05'$	3°47′	$\theta_{70} = 5°30'30''$ $\theta_{90} = 6°30'00''$	$\theta_{E_1^6} = 61°35'00''$	619, 5 733, 5	9129	33±3	3°38′	$\theta_{70} = 5°35'45''$ $\theta_{84} = 6°17'00''$	$\theta_{E_1^6} = 62°14'30''$	629, 0 708, 5	9123	25±3
	15	$12\theta_{70} + 2\theta_H = 81°05'$	3°33′	$\theta_{70} = 5°38'45''$ $\theta_{90} = 6°40'00''$	$\theta_{E_1^7} = 74°25'00''$	634, 5 751, 5	9117	45±3	3°29′	$\theta_{70} = 5°41'30''$ $\theta_{84} = 6°23'30''$	$\theta_{E_1^7} = 74°41'30''$	640, 0 720, 0	9120	28±3
		$14\theta_{70} = 81°05'$	3°19′	$\theta_{70} = 5°47'30''$		651, 06	9114, 8	47, 2	3°19′	$\theta_{70} = 5°47'30''$		651, 06	9114, 8	32, 8
8 Ion. reflect.		$16\theta_H = 81°05'$	6°28′	$\theta_{90} = 5°04'04''$	$\theta_{E_1^1} = 5°04'04''$	574, 38	9190, 1	0	5°53′	$\theta_{84} = 5°04'04''$	$\theta_{E_1^1} = 5°04'04''$	573, 21	9171, 4	0
		$16\theta_{70} = 81°05'$	4°35′	$\theta_{70} = 5°04'04''$		570, 72	9131, 5	58, 6	4°35′	$\theta_{70} = 5°04'04''$		570, 72	9131, 5	39, 9

flections" for instance shows first the relation between geocentrical angles for the paths 1 and 6 (night and day propagation) as well as 2, 3, 4, and 5 relating to so-called intermediate propagations, figure 13. Then angles of incidence ϕ on the ground, geocentrical angles θ_{70}, θ_{90} respectively θ_{84}, as well as the geocentrical angle for the last night hop with respect to Neuchâtel, $\theta_{E_1^i}$ ($i=1, 2, \ldots 5$), are presented, s is the length of the path from one reflection point on the ground to the next following on the lower edge of the ionosphere. $S=\Sigma s$ the total length of each peculiar path 1, 2, 3, 4, 5, and 6, figure 13, ΔS being the difference in the length of each one of them with the length of path 1.

Figure 12 illustrates the graphical method used to determine the above elements. The functions $s=f(\theta)$ and $s=f(\phi)$ are given for three different altitudes. A third diagram ($\theta_{70}-\theta_{84,\,90}$) shows the constructed curves $\phi_{70,\,90}$ and $\phi_{70,\,84}$, locus of points such that for the corresponding ϕ_{70} and $\phi_{84,\,90}$ angles of incidence on the ground ϕ_{70} and $\phi_{84,\,90}$ are equal (see graphical construction of the angles of incidence $\phi_{70,\,90}$, respectively $\phi_{70,\,84}=0°$ and $\phi_{70,\,90}$, respectively $\phi_{70,\,84}=4°$). The straight lines numbered 1 to 15 are the relation between geocentrical angles with regard to the geocentrical angle Neuchâtel-Balboa. Each bundle of straight lines represents one mode of propagation.

The following example is an illustration of the method, figure 12: the straight line 9 intersects the curve $\phi_{70,\,90}$ at K in the diagram ($\theta_{70}-\theta_{84,\,90}$). K is first related to the abscissa $\theta_{84,\,90}$ where $\theta_{90}=7°38'45''$ is found; afterward $s_{90}=860{,}0$ km is read on the curve $H=90$ km in the diagram ($s-\theta$). This value on the corresponding curve $H=90$ km in the diagram ($s-\phi$) yields the angle of incidence on the ground $\phi=2°02'$ on the abscissa. The path length $s_{70}=738{,}0$ km is found by intersecting the projection line with the curve $H=70$ km in the diagram (s,ϕ). Returning to diagram (s,θ), θ_{70} is found to be $6°34'45''$.

This method has the advantage of being quick. It can furthermore be applied to all propagation modes, provides of course, that the straight line equations are adapted first to the geocentrical angles as given by the locations of both transmitter and receiver. The graphical method just described is, of course, not as accurate as the mathematical method. Night and day path lengths for each mode 5, 6, 7, and 8 were accurately calculated. Global differences between night and day paths are therefore known with sufficient accuracy, while partial differences between intermediate path lengths are far less accurate since they were found with the above graphical method.

b. Determination of the Mode

It was established in section 3.2 that length differences of the path traveled by the NBA signal varied between 14,7 km and 21,3 km for day and night propagation.

If it is now assumed that night reflection occurs at an altitude of 90 km and day reflection at 70 km according to table 2, a difference of 31,5 km for 5 hops, 39,1 km for 6 hops, 47,2 km for 7 hops, and 58,6 km for 8 hops is found. For a reflection altitude of only 84 km during the night, these differences are respectively 21,6 km, 26,8 km, 32,8 km, and 39,9 km. It may be noted that on the registration of April 22–23, 1961, figure 10, the difference $\Delta S=21{,}3$ km is similar to that for 5 hops with a reflection altitude of 84 km. Inferred differences for the examples of September 7, 1960, figure 6; and September 11, 1960, figure 8; yield reflection altitudes of about 82 and 80 km for the same mode.

Consequently, it seems fairly well established that mode 5 is the actual propagation mode of the NBA signal between Balboa and Neuchâtel.

The problem has to be considered more closely, however. Assume, for instance, a propagation of mode n during the night (n hops) and a propagation of mode $n+1$ during the day ($n+1$ hops) or inversely. It becomes immediately obvious that the eventuality of having a mode $n+1$ during darkness and n during daylight must be eliminated, the resulting differences of path lengths ΔS being far higher than those deduced from the registrations. The other eventuality, n ionospheric hops during darkness and $n+1$ hops during daylight, is more logical and looks tempting at first sight.

A scrutiny of the global differences of the traveled paths for $H=90$ km and $H=84$ km (as extracted from table 2) shows the following:

5 night reflections / 6 day reflections: $\Delta S_{90}=9116{,}5-9099{,}3=17{,}2$ km; $\Delta S_{84}=9106{,}6-9099{,}3=7{,}3$ km

6 night reflections / 7 day reflections: $\Delta S_{90}=9138{,}4-9114{,}8=23{,}6$ km; $\Delta S_{84}=9126{,}0-9114{,}8=11{,}2$ km

7 night reflections / 8 day reflections: $\Delta S_{90}=9162{,}0-9131{,}5=30{,}5$ km; $\Delta S_{84}=9147{,}6-9131{,}5=16{,}1$ km.

The differences thus calculated correspond closely to those deduced from the recordings, especially for 17,2 and 23,6 km.

However, transition from one mode to another can only take place in a precise order.

If an intermediate propagation of mode n (n ionospheric reflections) is considered, n_D being the number of day reflection points and n_N the number of night reflection points, the following relation obviously applies:

$$n=n_D+n_N.$$

The mode of next higher order would be

$$n'=n+1.$$

Transition from mode n to n' must follow the law

$$n'=(n_D+1)+n_N$$

where $n_D+1=n_D'$, number of day reflections for mode n'.

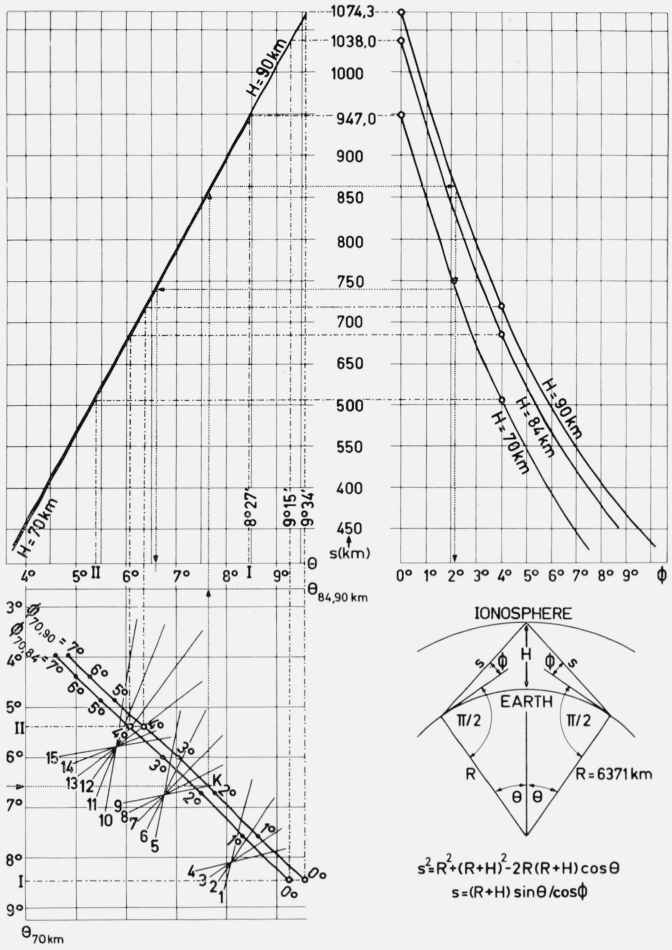

FIGURE 12. *Graphical method to find the angle of incidence ϕ, the distance s between the ionospheric reflection point and the next ground reflection point, and the corresponding geocentrical angle θ for a determined mode of propagation that is represented by a bundle of straight lines.*

LEGEND: equations of the straight lines for

5 ionospheric reflections
1: $2\theta_{70}+8\theta_{84,90}=81°05'$
2: $4\theta_{70}+6\theta_{84,90}=81°05'$
3: $6\theta_{70}+4\theta_{84,90}=81°05'$
4: $8\theta_{70}+2\theta_{84,90}=81°05'$

6 ionospheric reflections
5: $2\theta_{70}+10\theta_{84,90}=81°05'$
6: $4\theta_{70}+8\theta_{84,90}=81°05'$
7: $6\theta_{70}+6\theta_{84,90}=81°05'$
8: $8\theta_{70}+4\theta_{84,90}=81°05'$
9: $10\theta_{70}+2\theta_{84,90}=81°05'$

7 ionospheric reflections
10: $2\theta_{70}+12\theta_{84,90}=81°05'$
11: $4\theta_{70}+10\theta_{84,90}=81°05'$
12: $6\theta_{70}+8\theta_{84,90}=81°05'$
13: $8\theta_{70}+6\theta_{84,90}=81°05'$
14: $10\theta_{70}+4\theta_{84,90}=81°05'$
15: $12\theta_{70}+2\theta_{84,90}=81°05'$

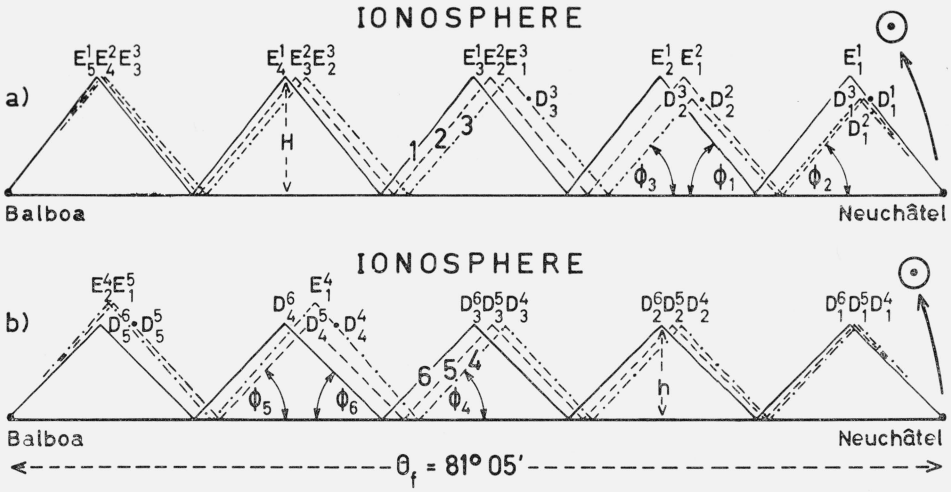

FIGURE 13.—*Geometrical model of the longwave propagation about sunrise in the case of a 5-hop skywave for the distance Balboa-Neuchâtel (night propagation 1, intermediate propagation 2. 3. 4. 5, day propagation 6).*

Figure 13 shows this behavior more explicitly. Path 3 for instance (intermediate propagation 3) involves 2 day (D_1^3 and D_2^3) and 3 night reflection points (E_1^3, E_2^3, and E_3^3), so that

$$\begin{aligned} n_D &= 2 \\ n_N &= 3 \\ n &= 5. \end{aligned}$$

The transition to $n'=6$ ionospheric hops will be such that

$$\begin{aligned} n_D' &= (n_D+1) = 3 \\ n_N' &= n_N \quad\quad = 3 \\ n' &= n+1 \quad\quad = 6 \end{aligned}$$

because the decrease of the altitude of the last night reflection point E_1^3 occurs simultaneously with the addition of a new reflection point to the remaining.

In table 2, path 3 discussed above is shown by (2) (No. 2 in fig. 12) while (7) (No. 7 in fig. 12) expresses the transition.

What now are the effects of a transition, in accordance with the law indicated above from mode n to n' on the behavior of S, the length of the path traveled by the signal? Table 2 shows that whatever the altitude of the night reflection chosen (H=90 or 84 km) and regardless of the timing of the transition from one mode n to the next higher mode $n'=n+1$, the length of the path S increases. Inversely, if a night as well as a day propagation are of the same mode (e.g., paths 1, 2, 3, 4, 5, and 6, fig. 13, and table 2) (5 hops), the length of the path is always shorter than that immediately preceding.

If, then, we assume a change of mode occurring together with sunrise over the path Neuchâtel-Balboa, a sudden increase in path length should take place at the moment of change of the mode.

The recordings, figures 6 to 10, however, show that the shift Δt_I of the sinusoid always occurs in the same direction at sunrise, respectively at sunset; therefore the respective variations ΔS of the path length traveled by the signal are similar. While at sunrise the length S of the path traveled decreases more or less evenly showing no tendency to increase at any time, at sunset, on the other hand, the length increases with no sign of decrease at any time.

It can be concluded accordingly, that the mode of NBA signal propagation is the same both at day and at night. Mode five is therefore found to be applicable, altitudes of reflection points being about 70 km during daylight and between 80 and 84 km at night according to the recordings available, figures 6, 8, and 10.

Angles of incidence on the ground for a five-hop mode in table 2, for a day altitude of 70 and 84 km at night, then, are

$$0°27' \leq \phi \leq 1°14'.$$

4.4. Consideration on the Night Reflection Altitudes of the GBR and NBA Signals

The night reflection altitudes of the GBR signal were found to be higher than those of the NBA signal.

Since both frequencies (16 kc/s for Rugby, 18 kc/s for Balboa) are quite close to each other, night reflection altitudes would be equal for identical geometrical propagation conditions. This being not the case, the inequality

$$\theta_{E_1^3}|(\text{Balboa}) > \theta_E|(\text{Rugby})$$

must be borne in mind.

This implies that angles of incidence on the lower edge of the ionospheric layer are also unequal: the GBR signal will penetrate further into the ionosphere and reflect at a higher altitude than the NBA signal.

5. Introduction to the Detailed Study of the Geometrical Model of Longwave Propagation at Sunrise and Sunset

The recordings for Rugby reveal a sudden translation of the sinusoid on the oscilloscope screen from I to M at sunrise, figures 3 and 5. On the other hand, sunrise recordings for Balboa are different in this respect. On April 23, 1961 for instance, 5 successive shifts numbered 1 to 5 in figure 10 are shown.

The question as to the relation between the sudden shifts of the sinusoid and the ionospheric reflection points now arises, since the altitude decrease of each of them must result in a shift of the sinusoid on the oscilloscope screen. A correlation between the times of sunrise at the reflection points and the times at which the shifts occur could be searched. However, computing a sunrise time at a reflection point is equivalent to a computation of the zenithal distance Z of the sun at this point. This new notion will furthermore be used to fix similar singularities of possibly identical origin on various recordings as will be shown later. It can be assumed that similar singularities related to the same reflection point, but taken successively on different recordings must by necessity have equal zenithal distances. When computed under identical conditions for several reflection points in a multihop mode propagation, similar zenithal distances will again be found both for sunrise and sunset. The zenithal distance would therefore appear to be independent of the declination of the sun and the position of the reflection point. This is not unlikely, since the rate of production of electrons in the ionosphere is known to vary with the cosine of the zenithal distance of the sun.

This is the approach to the detailed study of the proposed model, figure 13, which will also clarify the model related to sunset, figure 14.

6. Geometrical Considerations

6.1. Rugby

It is established in section 4.2 that the mode of the GBR signal propagation is only a one-hop mode. Let N be the midpoint of the arc of great circle joining Neuchâtel and Rugby along the ground, figure 11, D the day and E the night reflection points. Starting from the coordinates of Rugby (52°22′ N—01°11′ W) and Neuchâtel (47°00′ N—06°57′ E), it is found that

N (49°16′ N—03°16′ E),
D (49°16′ N—03°16′ E—70 km),
E (49°16′ N—03°16′ E—88 km),

with $\theta_f=7°30'$, the geocentrical angle between the receiver and the transmitter

$$\theta_E=\theta_D=\theta_N=\frac{\theta_f}{2}=3°45',$$

the azimuth of Rugby from Neuchâtel being

$$A_Z=318°37'.$$

The recordings, figures 2, 3, 4, and 5, had shown an altitude of the night reflection layer varying between 88 and 91 km (see sec. 4.2). This altitude was selected at 88 km for subsequent computations.

6.2. Balboa

a. Sunrise

The intermediate propagation (paths 2, 3, 4, and 5, fig. 13) requires the reflection points on the ionospheric layer contained in table 3 (azimuth $A_Z=273°44'$).

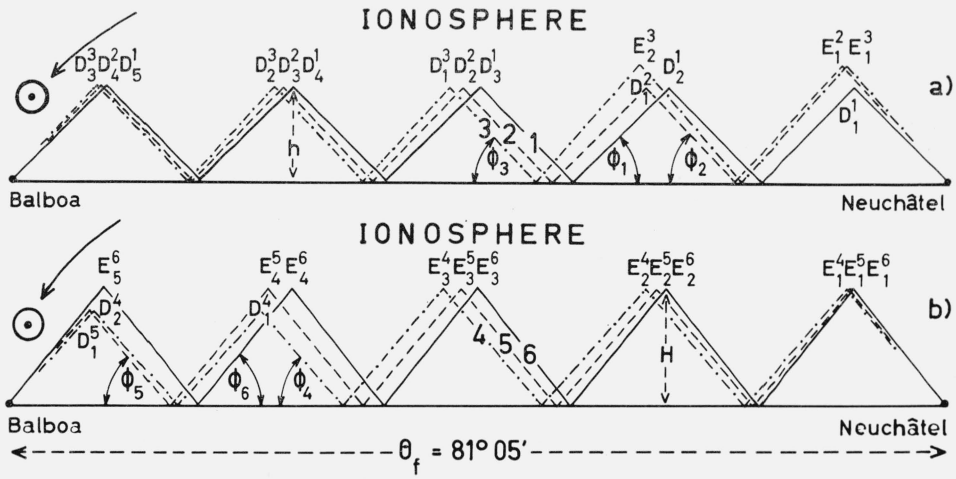

FIGURE 14. *Geometrical model of the longwave propagation about sunset in the case of a 5-hop skywave for the distance Balboa-Neuchâtel (day propagation 1, intermediate propagation 2. 3. 4. 5, night propagation 6).*

The geocentrical angles $\theta_{E_1^1} \ldots \theta_{E_1^5}$ formed by each of the points $E_1^1 \ldots E_1^5$ tabulated between the two diagonals of table 3 with the receiver (Neuchâtel) were calculated in table 2 on the basis of the geocentrical angles θ_{70} and θ_{84} found with the graphical method already described, figure 12.

TABLE 3

Path	Reflection point				
1	E_1^1	E_2^1	E_3^1	E_4^1	E_5^1
2	D_1^2	E_1^2	E_2^2	E_3^2	E_4^2
3	D_1^3	D_2^3	E_1^3	E_2^3	E_3^3
4	D_1^4	D_2^4	D_3^4	E_1^4	E_2^4
5	D_1^5	D_2^5	D_3^5	D_4^5	E_1^5
6	D_1^6	D_2^6	D_3^6	D_4^6	D_5^6

In a previous study [Rieker 1960, sec. 2.2 and 2.13], a simple method of computation of these geocentrical angles was evolved, their general expression being

$$\left(\theta_{E_1^1}\right)_L = \frac{\theta_f}{2n},$$

$$\left(\theta_{E_1^m}\right)_L = \frac{(2m-1)}{2n}\theta_f - \frac{\alpha[n-(m-1)]}{n}(2m-1)+\alpha,$$

$$\left(\theta_{D_{m-1}^m}\right)_L = \left(\theta_{D_m^m}\right)_L \frac{2m-3}{2m-1},$$

$$\left(\theta_{D_n^{n+1}}\right)_L = \theta_f - \frac{\theta_f}{2n}, \qquad (5)$$

where α is defined by the relation

$$\left(\theta_{E_1^m}\right)_L - \left(\theta_{D_m^m}\right)_L = \alpha,$$

for our case $\alpha \cong 0°45'$, n being the number of ionospheric reflections ($n=5$ in our case, see sec. 4.3b), $\theta_f = 81°05'$ the geocentrical angle between the transmitter (Balboa) and the receiver (Neuchâtel); m an integer defined by the inequality $1 < m \leq n$, the index L relating the expressions to sunrise.

When the azimuth and geocentrical angle of each characteristical point tabulated between the diagonals of table 3 are known, the coordinates λ and φ of each point can be computed easily; these are shown in tables 4 and 5.

The recordings (figs. 6, 8, 10) yielded altitudes of night reflection varying between 80 and 84 km (see sec. 4.3b); a value of 84 km was selected for further computations.

TABLE 4

Reflection point $H=84$ km	θ $A_z=273°44'$	φ	λ
E_1^1	8°07′	46°55′N	4°56′W
E_1^2	23 16	43 40	26 03
E_1^3	39 03	36 42	44 38
E_1^4	55 23	27 00	60 11
E_1^5	72 22	15 26	73 34

TABLE 5

Reflection point $h=70$ km	θ $A_z=273°44'$	φ	λ
D_1^2	7°31′	46°59′N	4°05′W
D_2^3	22 59	43 45	25 41
D_3^4	39 03	36 42	44 38
D_4^5	55 43	26 47	60 28
D_5^6	72 58	14 52	73 53

b. Sunset

It was shown in section 4.3 that a five-hop mode must be applied to the Balboa-Neuchâtel transmissions. This involves consideration of an intermediate propagation 2, 3, 4, and 5 for the transition from day to night propagation similar to the case of sunrise considered previously, assuming angles of incidence on the ground for each particular path 1, 2, 3, 4, 5, or 6, figure 14 to be identical.

Table 6 shows all sunset reflection points. By reasons of symmetry the geocentrical angles between Neuchâtel and the reflection points tabulated between the two diagonals of table 6 can be derived from (5):

$$\left(\theta_{D_1^1}\right)_C = \frac{\theta_f}{2n}$$

$$\left(\theta_{D_1^{n+2-m}}\right)_C = \vartheta_f - \frac{2m-3}{2m-1}\left(\theta_{D_m^m}\right)_L$$

$$\left(\theta_{E_{n+1-m}^{n+2-m}}\right)_C = \vartheta_f - \left(\theta_{E_1^m}\right)_L$$

$$\left(\theta_{E_n^{n+1}}\right)_C = \theta_f - \frac{\theta_f}{2n} \qquad (6)$$

where, as previously in the case of sunrise,

$$1 < m \leq n$$

n being the number of ionospheric reflections and m an integer, the index C relating the expressions to sunset.

The azimuth $A_Z = 273°44'$ and the geocentrical angle of the characteristical reflection points with

respect to Neuchâtel being known, the coordinates λ and φ of each of them can be computed easily. These are shown in tables 7 and 8.

TABLE 6

Path	Reflection point				
1	D_1^1	D_2^1	D_3^1	D_4^1	D_5^1
2	E_1^2	D_1^2	D_2^2	D_3^2	D_4^2
3	E_1^3	E_2^3	D_1^3	D_2^3	D_3^3
4	E_1^4	E_2^4	E_3^4	D_1^4	D_2^4
5	E_1^5	E_2^5	E_3^5	E_4^5	D_1^5
6	E_1^6	E_2^6	E_3^6	E_4^6	E_5^6

TABLE 7

Reflection point h=70 km	θ A_z=273°44′	φ	λ
D_1^1	8°07′	46°55′N	4°56′W
D_1^2	25 22	42 55	28 45
D_1^3	42 03	35 04	47 43
D_1^4	58 06	25 14	62 29
D_1^5	73 34	14 35	74 27

TABLE 8

Reflection point H=84 km	θ A_z=273°44′	φ	λ
E_1^2	8°43′	46°53′N	5°50′W
E_2^3	25 42	42 40	29 06
E_3^4	42 03	35 04	47 43
E_4^5	57 49	25 25	62 15
E_5^6	72 58	14 52	73 53

7. Further Developments

7.1. Methods

a. Introduction

Prior to the detailed study of individual recordings, a summary of the three variables used in their interpretation and the methods of their computation follows:

The zenithal distance Z of the sun,
the times of rising and setting of the ionizing radiation of the sun,
the distance d between one ionospheric reflection point and the layer formed by the ionizing radiations of the sun.

b. Determination of the Zenithal Distance of the Sun

The following computation method was used to determine the zenithal distance Z of the sun for a given time T and an ionospheric reflection point E respectively D of coordinates (λ, φ, h), figure 15; from

$$\cos U=\frac{R}{R+h}$$

where

U=angle of depression
R=radius of the earth=6371 km

and

$$-\sin U=\sin\delta\sin\varphi+\cos\delta\cos\varphi\cos(t_0+t), \quad (7)$$

the value of

$$(t_0+t)_{L,C}$$

is calculated for sunrise L or sunset C at point E or D of coordinates (λ, φ, h).

δ is the declination of the sun, t_0 the hour angle of the sun at sunrise or sunset, t the time period between either sunrise or sunset and the time considered.

For a known time difference

$$L-T \text{ or } C-T$$

the following is derived easily:

at sunrise

$$(t_0+t)_T=(t_0+t)_L+(L-T)$$

at sunset

$$(t_0+t)_T=(t_0+t)_C-(C-T)$$

The zenithal distance is given by

$$\cos Z=\sin\delta\sin\varphi+\cos\delta\cos\varphi\cos(t_0+t)_T. \quad (8)$$

c. Determination of the Time of Rising or Setting of the Ionizing Radiation of the Sun

Sunrise or sunset at any given point (λ, φ, h) near the surface of the earth is associated normally to the appearance or disappearance of the solar disk in the visible spectrum. However, the main ionizing agent of the high atmosphere is the ultraviolet radiation of the sun of below about 3000 A; it is logical, therefore, to assume a photoionic effect of this radiation on the air-components of the high atmosphere, when investigating the relationship existing between the times of sunrise or sunset at points along the path of a signal and the times at which phase fluctuations of this signal appear on the recordings. It is also known that this ultraviolet radiation is completely absorbed by the ozone layer. In other words, this means that this ultraviolet radiation will reach the point (λ, φ, h) after the sun has risen and will leave it before the sun has set in the visible spectrum. The problem is, therefore, reduced to a computation of the times of sunrise and sunset in the visible spectrum referring to a sphere with a radius of $R+\Delta_r$ reaching the

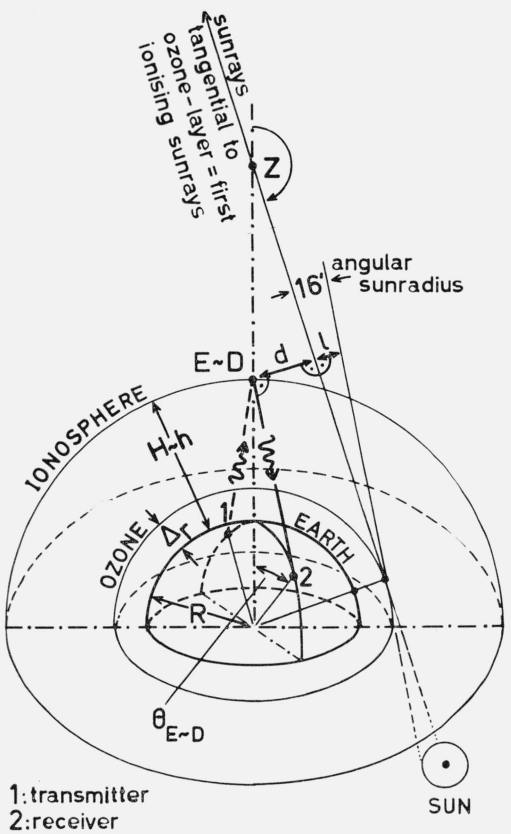

FIGURE 15. *One-hop skywave: zenithal distance* Z *and distance* d *from the reflection point* E *or* D *to the surface formed by the ionizing rays which are tangential to the ozone layer.*

sphere of influence of the ozone layer. The introduction of the notion of the rising and setting of the ionizing radiation of the sun is thus justified.

A simple computation method for the time difference results from a known altitude Δ_r of the sphere of influence of the ozone layer above the surface of the earth. Starting from the equations

$$\cos U_1 = \frac{R}{R+h} \text{ and } \cos U_2 = \frac{R+\Delta_r}{R+h},$$

where U_1 and U_2 are the angles of depression, R the radius of the earth=6371 km and h the altitude of the point under study.

Equation (7) then yields the difference of the times

$$|(t_0+t_1)-(t_0+t_2)|=\Delta.$$

The time at which the ionizing radiation rises at an ionospheric reflection point thus becomes

$$L+\Delta,$$

the time of their setting becoming

$$C-\Delta.$$

The altitude Δ_r being difficult to determine on the recordings under study, reference was made to a previous study [Rieker, 1960, sec. 1.3] where it was found to be 28 km; this value was adopted for further use in the present study.

d. Computation of the Distance *d* From One Ionospheric Reflection Point to the Layer Formed by the Ionizing Radiations of the Sun

Some phase fluctuations of the GBR or NBA signal occur before the ionizing radiations of the sun have risen at the corresponding reflection point (λ, φ, h). In this case the distance d from the reflection point to the layer formed by the ionizing radiations has been calculated, figure 15.

When, at sunrise, the phase fluctuation of the signal occurs before the ionizing radiations of the sun reach the reflection point considered, the rate of electron density must have been modified before the said radiations reached the particular reflection point.

The layer formed by the ionizing radiations issuing from the sun taken as a punctiform light source assumes, in the first approximation, the shape of a cylinder tangential to the ozonosphere and therefore to the sphere $R+\Delta_r$, figure 15.

It is easily recognized that for a ionospheric reflection point E respectively D, d is defined by the equation

$$d=(R+\Delta_r)-(R+h)\sin Z. \qquad (9)$$

Z is the zenithal distance of the sun at the day or night reflection point considered; it should not be mistaken for the zenithal distance of the sun at Neuchâtel at the same moment, which would have an altogether different value.

If, for curiosity's sake, the solar disk in the visible spectrum is assumed to have a diameter of 16′, the distance d would have to be corrected by a value l determined by the expression (see fig. 15):

$$l=(R+h)\cos(\pi-Z)tg\ 16'. \qquad (10)$$

Assuming that:

d=100 km
Δ_r=28 km:altitude of the sphere of influence of the ozone layer [Rieker, 1960, sec. 1.3]
R=6371 km:radius of the earth
h=88 km:altitude of the reflection point (see sec. 6.1),

it is found that

$Z=102°47'$
l=6,6 km.

Conversely, the variation of Z resulting from d=6,6 km is $Z\cong 15'$.

As will be shown in the next paragraph, this error can be neglected, the inaccuracies resulting from the readings taken on the recordings being of the same

order of magnitude, sometimes even more important. The sun can therefore be taken as a point light source. It might be added that a strict reasoning would involve the dimensions of the sun in the ultraviolet.

7.2. Interpretation of the Recordings

a. Introduction

The Rugby recordings will be studied first, figures 2 to 5, followed by the more complex recording from Balboa, figures 6 to 10. Recordings at sunrise being easier to interpret, they will be examined first.

Mention has already been made of the fact that these recordings were not made with the specific view of studying long wave propagation. This explains the interruption in the recordings of September 8 and 12, 1960, figures 7 and 9, before the sun had risen over the whole path Neuchâtel-Balboa. Furthermore, since these recordings were part of the initial trials conducted at the Neuchâtel Observatory, two different speeds of advance of the 35 mm film were used; on the original high speed recordings, figures 2, 3, 6, 7, 8, and 9, 1 mm represents 2 min, while on the low speed recordings, figures 4, 5, and 10, 1 mm corresponds to 8, 5 min. A reading error of 1 min results in an error for Z of $\Delta Z \cong 30'$ in the first case, while on the low speed recordings, a reading error of 4 min results in an error of $\Delta Z \cong 1°$ to 2°.

The "Tables Crépusulaires" [Lugeon 1934, 1957] were used to compute the times of sunrise and sunset at a point (λ, φ, h).

It should be mentioned finally that the January 24 and 25, 1961 recordings, figures 4 and 5, were used earlier in a preliminary study [Rieker, 1961].

b. Interpretation of the Recordings of the Rugby GBR Signal

Recordings of September 11, 1960, Figure 3 and January 25, 1961, Figure 5 at Sunrise. In spite of two different time scales having been used (abscissa), both recordings show a sudden initial phase shift at I followed by a clearly marked stabilization at K in figure 3 and M in figure 5. From point M onward, no significant shifting of the phase occurs on both recordings. Table 9 shows the time of rising of the sun and of the ionizing radiation at the characteristic points N, D, and E defined in section 6.1, figure 11, as well as the corresponding zenithal distances Z defined in section 7.1b, figure 15.

TABLE 9

Place	Time of sunrise			Time of incidence of the first ionizing sunray		
	11. 9. 60 UT	25. 1. 61 UT	Z	11. 9. 60 UT	25. 1. 61 UT	Z
Neuchâtel	5h09m	7h11m	90°00′			
N	5 22	7 35	90 00			
D	4 28	6 37	98 27	4h40m	6h50m	96°33′
E	4 21	6 31	99 28	4 32	6 42	97 49

Table 10 comprises the results as computed for the times I, K, L, M indicated on figures 3 and 5. The zenithal distances Z of the sun at the times I, K, L, M were calculated at point N, figure 11 for both recordings. At a given time, K for instance, the zenithal distance is identical for all points on a vertical line from point N. The distance d between the night reflection point E (49°16′ N—03°16′ E—88 km) and the layer formed by the ionizing radiations was calculated for the time I (see sec. 7.1d, (9)).

TABLE 10

Sunrise

Abscissa in the figures 3 and 5	Reflection point	11. 9. 60			25. 1. 60		
		UT	Z	d	UT	Z	d
				km			km
I	E	4h29m	98°19′	8	6h39m	98°19′	8
K	D	4 40	96 33	0	6 57	95 30	------
L	D	5 03	92 59	------	------	------	------
M	D	5 31	88 27	------	7 37	89 42	------

The following considerations are based on table 10:

(1) On both recordings (September 11, 1960 and January 25, 1961), the initial shift of the phase occurs at a time corresponding to the time of rising of the ionizing radiation of the sun at point E (49°16′ N—03°16′ E—88 km).

(2) Both recordings show a singularity at the times K coinciding with a zenithal distance of the sun of about 96°.

Plotting A^2 ((3) sec. 2) below the January 25, 1961, recording as a time function calculated by repeated measurements of T' (μsec) an absorption curve showing the variation of the energy of the GBR signal is obtained. A minimum appears in this curve at time K which occurs at a reflection point altitude of about 82 km. Further singularities are noticeable in the absorption curve at times I and K.

(3) The singularity indicated at time L, figure 3, is not visible on the recording of figure 5. This fact is probably due to the slow speed of advance of the film.

(4) From time M onward i.e., when the ionizing radiation reaches the day reflection point D practically horizontally, the altitude of the point of the ionospheric reflection has nearly reached the lowest level. The received energy, on the other hand, has slightly increased again (see absorption curve, fig. 5).

Recordings of September 10, 1960, figure 2 and January 24, 1961, figure 4 at sunset. Phase fluctuations of the GBR signal are less clearly discernible at sunset than at sunrise. The recording of September 10, 1960, for instance, shows a very gradual phase shift beginning at time A, whereas the beginning of the phase shift is slightly clearer on the recording for January 24, 1961. The phase shift, furthermore, extends over a much longer period of time at sunset than at sunrise and generally appears to be more complex. Beginning at time G, however, the phase shift becomes very small. The increase of the altitude of the night reflection point is probably terminated at this time G.

As previously for sunrise, times of setting of the sun and of the ionizing radiation as well as the zenithal distances Z of the sun as computed for the characteristical points N, D, E defined in section 6.1 are presented in table 11.

TABLE 11

Place	Time of sunset			Time of incidence of the last ionizing sunray		
	10.9.60 UT	24.1.61 UT	Z	10.9.60 UT	24.1.61 UT	Z
Neuchâtel	17^h49^m	16^h17^m	90°00′			
N	18 06	16 22	90 00			
D	18 59	17 19	98 27	18^h47^m	17^h07^m	96°33′
E	19 06	17 26	99 28	18 56	17 15	97 49

Table 12 comprises the zenithal distances of the sun and the distances d from point E (49°16′N—03°16′E—88 km) to the layer formed by the ionizing radiations at times A, B, C, F, G indicating singularities apparent on the recordings.

The following considerations are based on table 12:

(1) At times A, figures 2 and 4, the zenithal distance is about 90° for both recordings. From that time onward the phase shift becomes apparent, i.e., the reflection point altitude begins to increase.

(2) When the zenithal distance approaches 94°, the phase shift of the GBR signal becomes slower.

(3) A singularity seems to be significant at time C on the September 10, 1960 recording, figure 2, this particular time C being the time of setting of the ionizing radiation of the sun at point E (49°16′N—03°16′E—88 km). This singularity does not appear on the recording of January 24, 1961, figure 4, or is at best only barely recognizable.

(4) When the zenithal distance reaches about 102°, a new singularity appears in the phase shift (time F). The distance from point E to the layer formed by the ionizing radiations then is about 100 km.

(5) Beginning at times G, the altitude increase of the night reflection point seems to be completed. It should be pointed out here that the zenithal distance of the sun and the distance from point E to the layer formed by the ionizing radiations on September 10, 1960, and January 24, 1961, are too dissimilar to postulate the existence of a relation between the two.

(6) By plotting A^2 ((3) sec. 2) below the recording of figure 4 as a time function, deduced from repeated measurements of T', respectively T'' (μsec), it would appear that critical points on the absorption curve are associated with times A, B, F. At time B a momentary increase of reflection capacity is noticeable. The reflection point would then have reached an approximate altitude of 73 km. Near time F absorption would have diminished considerably.

Discussion. A first conclusion attained by comparison of the results obtained at sunrise and sunset is that the altitude of the ionospheric reflection point is around 70 km as long as the zenithal distance of the sun lies between 0 and 90°. Zenithal distances at time A at sunset and time M at sunrise are about 90° according to tables 10 and 12.

TABLE 12

Sunset

Abscissa in the figures 2 and 4	Reflection point	10.9.60			24.1.61		
		UT	Z	d	UT	Z	d
				km			*km*
A	D	18^h06^m	90°00′	------	16^h16^m	89°29′	------
B	D	18 27	93 26	------	16 55	94 45	------
C	E	18 58	98 19	8	----------	----------	----------
F	E	19 30	103 06	108	17 41	101 41	74
G	E	22 48	125 09	1118	18 50	112 42	440

At sunrise, the phase shift seems to be triggered by the rising of ionizing radiations at point E (49°16′N—03°16′N—88 km), the beginning of the phase shift occurring at times I.

At sunset, the layer formed by the ionizing radiations again seems to be of same importance, the distance of the night reflection point E from this layer being about 100 km at times F while the ionizing radiations disappear at time C, figure 2.

The significance of the singularities noticed at the intermediate times K (sunrise) and B, F, G (sunset) becomes evident when related to the behavior of the energy A^2, figures 4 and 5.

When several ionospheric reflections (multihop mode) of the signal occur, the phase shifts which are completed in a relatively short time at sunrise, will be easily dissociated and analyzed. At sunset, on the other hand, the phase shift continues over a longer time, so that the interpretation of the recordings is more difficult; each peculiar phase shift produced by a successive increase of altitude of the reflection points being entangled with the next one.

c. Interpretations of the Recordings of the Balboa NBA Signal

Recordings of September 8, 1960, Figure 7; September 12, 1960, Figure 9; and April 23, 1961, Figure 10 at Sunrise

Unfortunately, the September 8, 1960, figure 7; and September 12, 1960, figure 9 recordings were terminated before sunrise had occurred over the whole path Neuchâtel-Balboa. The recording of April 23, 1961, figure 10, on the other hand, is completed. Two different speeds of advance of the film were also used.

A first examination of the recordings of the NBA signal at sunrise shows a jerky shifting of the phase; the April 23, 1961 recording looks rather like a flight of five steps. It will be shown that each step is associated with a decrease in the altitude of a night reflection point on the ionosphere. Identical symbols were maintained for similar singularities on different steps, indexes referring to step numbers. These symbols are the same as those used previously in the recordings of the GBR signal and relate to the same singularities of the phase shift (sec. 7.2b).

Reference is made here to figure 13, giving a schematic description of the model used. The ionospheric reflection points involved in these computations are to be found between the diagonal

lines in table 3 (sec. 6.2a). Times of sunrise and of the rising of the ionizing radiation as well as corresponding zenithal distances of the sun were computed for each of the reflection points mentioned (table 13). The night reflection altitude had been selected at 84 km in section 6.2a.

Table 14 is a systematic collection of the singularities noted in the recorded phase shifts of the NBA signal. They were assigned the letters H_i, I_i, K_i, L_i, O_i, M_i (i=1,2,3,4,5), i being the number of the step studied.

The following considerations are based on table 14:

(1) Contrary to the results obtained from the phase shift of the GBR signal, a first phase shift occurs at times H_i prior to the shift at I_i. Table 14 shows that at the times H_i the zenithal distances computed for the reflection points E_1^i vary between 101 and 104° while the distances d from the reflection points E_1^i to the layer of ionizing radiation fluctuate between 60 and 150 km. On both recordings of September 8 and 12, 1960, the zenithal distances calculated for the times H_4 (08.30 UT, 08.37 UT) had to be eliminated since the recordings are interrupted at 08.30 UT. The computation was made to show that these singularities belong to the third step (singularity O_3).

(2) At times I_i corresponding to the rising of the ionizing radiation at reflection point E on the recordings of the GBR signal (sec. 7.2b.), the zenithal distances related to point E_1^i vary between 99 and 101°, the distances d to the layer formed by the ionizing radiations being between 6 and 93 km.

(3) At the times O_i or M_i, the zenithal distances related to the corresponding day reflection points D_1^2, D_2^3, D_3^4, D_4^5, D_5^6 are near 90°. This result corroborates the findings on the recordings of the GBR signal.

(4) The zenithal distances of the sun calculated at the intermediate times K_i and L_i are generally between 93 and 97°.

(5) The energy A^2 of the NBA signal ((3) sec. 1) was shown below the April 23, 1961, recording as a function of time. For reasons of convenience, A^2 was represented as the reciprocal function $1/A^2$ due to the large variations of this function. This curve shows that:

The decrease in the energy occurs only after 05 UT (time L_1). For that time, the zenithal distance of the sun at the day reflection point D_1^2 would be 92°48′, table 14. The absorption curve of this initial step cannot be compared to the corresponding curve for Rugby, figure 5.

Two relative minima are discernible at the times O_2 and M_2. These refer to the second step.

The third, fourth, and fifth minima occurring at the times O_3, O_4 and L_5 are associated to steps 3, 4, 5. Zenithal distances computed with respect to the corresponding day reflection points fluctuate between 92 and 93°.

The intermediate maxima in the energy occur generally between the times H_i and I_i; these times precede the rising of the ionizing radiations of the sun at the night reflection point E_1^i only shortly.

Recordings of September 7, 1960, Figure 6; September 11, 1960, Figure 8; and April 22, 1961, Figure 10 at Sunset

The shifting of the phase of the NBA signal is much smoother at sunset than at sunrise. The different steps so clearly discernible at sunrise are smoothed out to such an extent that an analysis of the recordings becomes quite contingent. This is easily understood by referring to the phase recording of the GBR signal at sunset, figures 2 and 4. Attention had already been drawn to the considerably longer time periods over which the phase shift took place at sunset as compared to sunrise. Applied to a multihop skywave, this means that the phase shift associated with the first reflection point at sunset is not terminated by the time the shifting associated with sunset at the second reflection point intervenes.

TABLE 13

Reflection point or place	Time of sunrise				Time of incidence of the first ionizing sunray			
	8.9.60 UT	12.9.60 UT	23.4.61 UT	Z	8.9.60 UT	12.9.60 UT	23.4.61 UT	Z
Neuchâtel	5h05m	5h11m	4h36m	90°00′				
E_1^1	4 57	5 03	4 24	99 15	5h07m	5h14m	4h36m	97°33′
D_1^2	4 59	5 04	4 26	98 27	5 10	5 16	4 39	96 33
E_1^2	6 28	6 31	5 59	99 15	6 38	6 41	6 10	97 33
D_2^3	6 31	6 36	6 02	98 27	6 42	6 47	6 13	96 33
E_1^3	7 53	7 56	7 30	99 15	8 02	8 05	7 39	97 33
D_3^4	7 57	8 00	7 35	98 27	8 07	8 10	7 45	96 13
E_1^4	9 05	9 07	8 50	99 15	9 13	9 15	8. 58	97 33
D_4^5	9 10	9 12	8 55	98 27	9 19	9 21	9 04	96 33
E_1^5	10 08	10 08	9 59	99 15	10 15	10 15	10 06	97. 33
L_5^6	10 13	10 13	10 05	98 27	10 21	10 21	10 13	96 33

TABLE 14

Abscissa in the figures 7, 9, and 10	Reflection point	Sunrise								
		8.9.60			12.9.60			23.4.61		
		UT	Z	d	UT	Z	d	UT	Z	d
				km			km			km
H_1	E_1^1	4h32m	103°13′	115	4h46m	101°56′	84	4h14m	100°43′	57
I_1	E_1^1	4 58	99 05	25	5 02	99 25	31	4 29	98 30	15
K_1	D_1^2	5 15	95 50	----	5 12	97 07	8	4 46	95 26	----
L_1	D_1^2	5 29	93 12	----	5 39	92 36	----	5 03	92 48	----
M_1	D_1^2	----	----	----	----	----	----	5 26	89 06	----
H_2	E_1^2	5 57	104 31	150	6 00	104 35	152	----	----	----
I_2	E_1^2	6 28	99 15	28	6 31	99 15	28	6 07	97 57	6
K_2	D_2^3	6 44	96 11	----	6 38	98 06	22	6 07	97 38	15
L_2	D_2^3	6 59	93 33	----	----	----	----	6 19	95 40	----
O_2	D_2^3	----	----	----	7 13	91 54	----	6 36	92 55	----
M_2	D_2^3	----	----	----	7 18	91 00	----	6 55	89 33	----
H_3	E_1^3	7 32	103 18	117	7 29	104 29	149	7 14	102 09	89
I_3	E_1^3	7 47	100 25	50	7 47	101 01	63	7 33	98 42	18
K_3	D_3^4	----	----	----	8 08	96 53	4	----	----	----
L_3	D_3^4	----	----	----	----	----	----	7 52	95 11	----
O_3	D_3^4	8 30	91 58	----	8 37	91 24	----	8 09	91 57	----
H_4	E_1^4	8 30	106 50	221	8 37	105 48	188	8 34	102 36	99
I_4	E_1^4							8 43	100 43	57
K_4	D_4^5	Interrupted record			Interrupted record			9 00	97 24	11
O_4	D_4^5							9 21	92 54	----
I_5	E_1^5							9 59	99 15	28
K_5	D_5^6							10 12	96 49	4
L_5	D_5^6							10 29	92 51	----
P_5	D_6^5							11 24	79 50	----

An overriding of phase shifts occurs resulting in smoother curves for sunset than for sunrise.

Nevertheless, a trial was attempted. Although results obtained may not be very well established, there are indications that the schematic model depicted in figure 14 may be fairly representative of reality. The reflection points considered are to be found between the diagonal lines of table 6.

Table 15 contains the times of rising of the ionizing radiations of the sun at each of the ionospheric reflection points mentioned (see fig. 14 and table 6) together with sunrise times at these points and related zenithal distances. The altitudes of the night reflection points had been selected at 84 km (sec. 6.2a).

The times designated by the symbols A_i^*, A_i, B_i, C_i, F_i, F_i^* and G_i^* (table 16) were selected whenever phase shift singularities were more or less apparent. Not all were chosen due to the fairly even variation of the recorded curves.

Examination of table 16 and the recordings, figures 6, 8, and 10 leads to the following considerations:

(1) Shifting of the phase of the NBA signal usually begins at times A_i (i=1,2,4) with zenithal distances of the sun with respect to the reflection points D_1^i near 90°.

(2) On the April 22, 1961 recording, figure 10, the initial phase shift occurs earlier at time A_1^*, when the zenithal distance of the sun is only 85,5°.

(3) The singularities found at times B_1 and B_2 are peculiar to the recording of September 11, 1960, figure 8. Relevant zenithal distances are near 94°.

(4) At the times C_i (i=1,2,3,5) zenithal distances fluctuate between 97 and 100°, distances d from the night reflection point to the layer formed by the ionizing radiations between 0 and 29 km. It can therefore be assumed that the times C_i are approximately the setting times of the ionizing radiation at the night reflection points E_1^2, respectively E_2^3, E_3^4, and E_5^6.

TABLE 15

Reflection point or place	Time of sunset				Time of incidence of the last ionizing sunray			
	7.9.60 UT	11.9.60 UT	22.4.61 UT	Z	7.9.60 UT	11.9.60 UT	22.4.61 UT	Z
Neuchâtel	17^h56^m	17^h47^m	18^h25^m	90°00′				
D_1^1	19 34	19 26	20 06	98 27	19^h22^m	19^h14^m	19^h53^m	96°33′
E_1^2	19 42	19 33	20 14	99 15	19 32	19 23	20 03	97 33
D_1^2	21 02	20 54	21 30	98 27	20 51	20 43	21 19	96 33
E_2^3	21 07	21 00	21 36	99 15	20 58	20 50	21 25	97 33
D_1^3	22 07	22 01	22 28	98 27	21 58	21 51	22 18	96 33
E_2^4	22 11	22 04	22 33	99 15	22 02	21 56	22 24	97 33
D_1^4	22 56	22 52	23 11	98 27	22 48	22 43	23 02	96 33
E_4^5	23 00	22 55	23 14	99 15	22 52	22 47	23 06	97 33
D_1^5	23 37	23 33	23 45	98 27	23 29	23 25	23 37	96 33
E_5^6	23 39	25 35	23 48	99 15	23 32	23 28	23 40	97 33

TABLE 16

Abscissa in the figures 6, 8, and 10	Reflection point	Sunset								
		7.9.60			11.9.60			22.4.61		
		UT	Z	d	UT	Z	d	UT	Z	d
				km			km			km
A_1*	D_1^1							18^h38^m	85°36′	
A_1	D_1^1	18^h47^m	90°39′							
B_1	D_1^1				19^h00^m	94°08′				
C_1	E_1^1	19 27	96 48		19 34	99 25	31	20 18	99 51	39
F_1	E_1^2	20 14	104 20	145						
A_2	D_1^2	20 14	89 48							
B_2	D_1^2				20 32	94 31				
C_2	E_2^3	21 02	98 22	13	20 56	96 49				
C_3	E_3^4	22 02	97 33	0				22 31	98 52	21
F_3	E_3^4				22 24	103 14	115			
A_4	D_1^4				22 24	92 11		22 31	89 46	
C_5	E_5^6							23 49	99 29	32
F_5	E_5^6	23 45	100 41	56	23 46	101 53	82			
F_5*	E_5^6	24 06	105 41	184						
G_5*	E_5^6							25 21	120 23	830
G_5	E_5^6							25 40	124 31	1080

(5) At the times F_1, F_3, and F_5 but only on the September 7, figure 6 and September 11, 1960, figure 8 recordings zenithal distances with respect to the night reflection points E_1^2, respectively E_3^4, E_5^6, vary between 101 and 104°; the distances d would then be of the order of 100 km.

(6) The times F_5^*, figure 6, G_5^* and G_5, figure 10 were indicated and relevant zenithal distances and distances d were computed, however, without permitting any significant conclusion.

(7) The energy of the NBA signal ((3) sec. 1), was plotted on the April 22, 1961 recording as a function of time (see sec. 7.3a, item 5). The energy decreases after about 17 UT when the zenithal distance of the sun with respect to the day reflection point D_1^1 becomes smaller than 85°. At time A_1^* ($Z=85°36'$), the function $1/A^2$ diminishes rapidly. A weak maximum is discernible at time C_1 as well as a bend at time $A_4=C_3$. This absorption curve shows a diminished energy during the time period between sunset at reflection point D_1^1 and sunset at the last reflection point D_1^5.

8. Conclusions

Computation of angles of incidence ϕ on the ground as well as the deduction of the altitude of the night reflection points were made possible by determination of the propagation modes of the GBR signal (Rugby) and of the NBA signal (Balboa). The altitude of the day reflection points was taken from literature. Angles of incidence on the ground for the NBA signal vary between 0°27′ and 1°14′. These angles are much smaller than those derived from actually accepted mathematical theories [Wait 1961, Wait and Conda 1961].

The detailed study of these propagation modes was made possible by introducing the zenithal distances of the sun. A good accord was shown to exist between the zenithal distances computed for times selected on recordings with respect to the reflection points determined by the model, figures 13 and 14. The validity of the model is corroborated by these relations. Zenithal distances of the sun show a recurrence of these values on various recordings:

(1) $Z \cong 90°$ is the zenithal distance at which the altitude of the reflection point begins to increase at sunset. The altitude of the reflection point reaches the day value at sunrise.

(2) $Z \cong 97°$ is the zenithal distance at which the onset of the ionizing radiation occurs at the night reflection points. An increased phase shift is frequently observed at this time.

(3) $Z \cong 103°$ (for sunrise on the Balboa recordings only) is the zenithal distance at which the layer formed by the ionizing radiations is still about 100 km distant from the night reflection point. This time marks the beginning of the phase shift of the NBA signal and is identical with the beginning decrease of the night reflection point altitude. The decrease of the altitude of the night reflection precedes the onset of the ionizing radiation of the sun and substantiates previous statements [Rieker 1960, sec. 3.5.2.3.].

The fact that a similar phenomenon does not occur on the GBR signal transmission is probably due to to the higher altitude of the night reflection point (see sec. 4.4).

At sunrise, the behavior of the energy generally reveals a pronounced absorption at the time at which the phase shift, resulting from the decrease of the altitude of one ionosphere reflection point is about half completed. This absorption maximum occurs for zenithal distances of the sun varying between 92 and 95°, figures 5 and 10.

At sunset, the energy reveals a minor maximum around 17 UT, figure 4, for a zenithal distance near 94°. The NBA signal recorded in figure 10 merely shows a weakening of the energy during sunset on the path Neuchâtel-Balboa.

The absorption curves plotted under the recordings of figures 4,5,10, and the zenithal distances included in the tables are only of a descriptive nature. The study of their behavior has facilitated the understanding of the relation existing between sunrise and sunset in the ionosphere and the propagation of longwaves. Now that the general behavior of this relation appears to be known qualitatively and that the close relationship with the energy and the phase shift has become obvious, a study of the detailed quantitative behavior of the energy would be very interesting. This study would require, so it seems, a more direct method of absorption measurement.

We record our gratitude to Dr. J. Bonanomi, Director of the Neuchâtel Cantonal Observatory, who made available the recordings as well as relevant technical data.

9. References

Bracewell, R. N., K. G. Budden, J. A. Ratcliffe, T. W. Straker, and K. Weekes (1951), The ionospheric propagation of low and very low frequency radiowaves over distances less than 1000 km, Proc. Inst. Elec. Engrs. **98** Part III.

Budden, K. G., J. A. Ratcliffe, and M. V. Wilkes (1939), Further investigation of very long waves reflected from the ionosphere, Proc. Roy. Soc., Ser. A, No. 944.

Gregory, J. B. (1956). Ionospheric reflection from heights below the *E*-region, Australian J. Phys. **9**, No. 3.

Helliwell, R. A., A. J. Mallinckrodt, and F. W. Kruse (1951), Fine structure of the lower ionosphere, J. Geophys. Res., No. 56.

Lugeon, J. (1934), Tables Crépusculaires, lère édition. République polonaise, Inst. Natl. Météorol., Warszawa.

Lugeon, J. (1957), Tables Crépusculaires, 2ème édition élargie. Acad. polonaise des Sciences, Varsovie.

Nertney, R. J. (1953), The lower *E* and *D* region of the ionosphere as deduced from long radiowave measurements, J. Atmospheric Terrest. Phys. **3.**

Revellio, K. (1956), Die atmosphärischen Störungen und ihre Anwendung zur Untersuchung der unteren Ionosphäre. Mitteilung aus dem Max-Planck-Institut für Physik der Stratosphäre, Weissenau b. Ravensburg.

Rieker, J. (1960), Le lever du soleil dans l'ionosphère et ses repercussions sur la propagation des ondes longues. Geofis. Pura Appl. **46,** Part II.

Rieker, J. (1961), Quelques considérations sur la propagation des ondes longues au lever et au coucher du soleil. Actes Soc. Helv. Sci. Nat., Bienne.

Wait, J. R. (May 1959), Diurnal change of ionospheric heights deduced from phase velocity measurement at VLF. Proc. IRE, **47,** No. 5, 998.

Wait, J. R. (1961), A diffraction theory for LF sky-wave propagation J. Geophys. Res. **66,** No. 6, 1713–1724.

Wait, J. R. and A. Conda (1961), A diffraction theory for LF sky-wave propagation. An additional note, J. Geophys. Res. **66,** No. 6, 1725–1729.

Wait, J. R. (1962), Electromagnetic waves in stratified media, Pergamon Press, Oxford.

(Paper 67D2–249)